



## Chromium(VI) removal from aqueous solution using a new synthesized adsorbent

Qiuyi Wang<sup>a</sup>, Nan Chen<sup>a,b,\*</sup>, Yang Yu<sup>a</sup>, Chuanping Feng<sup>a,b</sup>, Qian Ning<sup>a</sup>, Weiwu Hu<sup>a,c</sup>

<sup>a</sup>School of Water Resources and Environment, China University of Geosciences, Beijing 100083, China, Tel. +86 15 512392681; email: [qiuyiwang926@gmail.com](mailto:qiuyiwang926@gmail.com) (Q. Wang), Tel. +86 10 82322281; Fax: +86 10 82321081; email: [cnjing2008@hotmail.com](mailto:cnjing2008@hotmail.com) (N. Chen), Tel. +86 18 010033186; email: [yuyang1914@gmail.com](mailto:yuyang1914@gmail.com) (Y. Yu), Tel. +86 13 801205306; email: [fengchuanping@gmail.com](mailto:fengchuanping@gmail.com) (C. Feng), Tel. +86 18 631102879; email: [ningqianhao@126.com](mailto:ningqianhao@126.com) (Q. Ning), Tel. +86 13 811783404; email: [huweiwu010@163.com](mailto:huweiwu010@163.com) (W. Hu)

<sup>b</sup>Key Laboratory of Groundwater Cycle and Environment Evolution, China University of Geosciences, Ministry of Education, Beijing, 100083, China

<sup>c</sup>The Journal Center, China University of Geosciences, Beijing 100083, China

Received 29 December 2013; Accepted 21 November 2014

### ABSTRACT

In order to effectively utilize agricultural wastes, the feasibility of using a novel calcined composite of dolomite, montmorillonite, and corn stover for removing chromium(VI) from aqueous solutions was examined. Batch experiments were conducted to investigate the effect of composite dosage, solution pH, initial concentration of chromium(VI), and temperature during the removal process. Chromium(VI) removal efficiency increased with increase in amount of the composite but remained almost unchanged (84–86%) when the solution pH increased from 2.0 to 11.0. The increase in chromium(VI) removal efficiency with increase in temperature from 20 to 40°C indicated that high temperature favored the removal process. This conclusion was also confirmed by adsorption energy evaluation where the reaction process was found to be endothermic and spontaneous. The removal process well fitted the pseudo-second-order kinetic model. Fitting of the experimental results with the intraparticle diffusion model revealed that the adsorption process was not controlled by the intraparticle diffusion. Isotherm studies demonstrated that the homogeneity of the composite surface and physical forces may more significantly affect the removal process.

*Keywords:* Chromium removal; Composite material; Dolomite; Montmorillonite; Corn stover

### 1. Introduction

Chromium is widely used in various industrial processes including mining, leather tanning, electroplating, and dyeing [1,2]. Consequently, the level of chromium in aqueous solutions has greatly increased

along with the discharge of these industrial plants, thereby posing a potential threat to the environment and human health [2]. Chromium(VI) is more toxic than chromium(III) because of the high solubility in almost the entire pH range and strong migration of the former [3]. Chromium(VI) mainly exists in the form of  $\text{CrO}_4^{2-}$ ,  $\text{HCrO}_7^-$ , and  $\text{Cr}_2\text{O}_7^{2-}$  species in aqueous solutions [4]. Hexavalent chromium is known to

\*Corresponding author.

be acutely carcinogenic, teratogenic, and mutagenic and is related to changes in plant morphology [5,6]. Given the public health risk, the World Health Organization has established an official reference dosage of 0.05 mg/L for chromium(VI) [7].

Traditional techniques used to remove Cr(VI) from aqueous solutions are reduction–precipitation [8–10], ion-exchange [11], membrane technology [12], and adsorption [13]. However, Barrera-Díaz et al. [10] has reported that an excess (50%) of the stoichiometric quantity of reducing agent is needed to achieve Cr(VI) removal. Meanwhile, the settling ability of floc and filterability of precipitated solids affect the performance of redox-assisted coagulation during chemical reduction [9]. Similarly, the main limitations of ion-exchange method are the potential fouling of resins and requirement of regular regeneration [11]. Hafiane et al. [12] reported that pretreatment, secondary pollution, high investment, and high operational costs are the most crucial weaknesses of membrane technologies.

Among these technologies, adsorption method is regarded as one of the most promising methods because of its low cost, low secondary pollution, simple design, and easy operation. The idea of treating chromium-contaminated solutions with natural minerals has been shown to be promising [14–17]. Numerous porous minerals exist in nature such as vermiculite, montmorillonite, and dolomite. Their adsorption capacity ascribed to their special structure enables their wide utilization in the industrial field [18]. Mineral materials exhibit unique properties for purification function including surface adsorption, porous filtration, defects of crystal structure, and ionic exchange [19]. Zeng et al. [3] used modified natural zeolite powder for removing Cr(VI) in solution with the capacity of 2.0 mg/g. Albadarin et al. [17] reported that Cr(VI) removal capacity of grounded dolomite can reach up to about 5.7 mg/g within 96 h. Sumathi et al. [20] explored column experiment packed with biological wastes and vermiculite mixture, and more than 90% Cr(VI) was removed. Dolomite, a natural mineral in Turkey, China, India, and Vietnam, is a major and cost-effective source of magnesium mostly used as an adsorbent to remove hazardous substances such as phosphate, arsenate, chromium, and copper ions from aqueous solutions [21,22]. The crystalline structure of dolomite contains alternative layers of  $\text{Ca}^{2+}$  and  $\text{Mg}^{2+}$  ions [23]. Montmorillonite is a dioctahedral smectite type (2:1) clay. It is abundant in nature and famous for its lamellar structure, high superficial area, and negative charges. So, montmorillonite is suitable for increasing stickiness in composite materials [16]. However, most articles are referred to a common drawback that powder adsorbent can easily cause obstruction in

practical application and is difficult to separate from liquid after adsorption. Chen et al. [24] has prepared a porous granular ceramic adsorbent by Knar clay, zeolite, and starch, performed effective in removing fluoride in subsequent operations and also can avoid clogging during field application. It has been reported that the pore texture on ceramic can be attributed to the sintering of starch during the calcination process. However, economically speaking, starch may not be the most appropriate material. Corn stover is a kind of abundant agricultural residual in China mostly used for cooking and heating in rural households with low efficiency [25]. Disposal of considerable corn stover also brings about serious environmental problem. Use of corn stover instead of starch for increasing pore texture will be tested in this research.

In this study, a novel calcined spherical granular composite ( $D=2\text{--}3\text{ mm}$ ) comprising dolomite, montmorillonite, and corn stover was developed. Montmorillonite is a suitable plasticizer because of its stickiness and ability to be controlled to any size [26]. It was utilized for molding granules to avoid the defects of filtration after adsorption. Corn stover was used to increase the porosity of the granular composite after calcination. To evaluate the performance of composites for Cr(VI) removal from aqueous solutions, the effects of contact time, pH, initial Cr(VI) concentration, adsorbent dosage, and temperature were investigated by batch experiments. Analyses of adsorption kinetics, isotherms, and thermodynamics were conducted and different models were utilized to explain the adsorption process of Cr(VI) on the solid–liquid system.

## 2. Materials and methods

### 2.1. Materials

Dolomite and montmorillonite materials (below 200 and 160 mesh, respectively) were purchased from Zhenyongwei Technology Development Co., Ltd. (Beijing, China). Corn stover was collected from Changping District (Beijing, China) and dried in an electric oven at  $45 \pm 2^\circ\text{C}$  for 48 h. These corn stovers were milled with a small high-speed smashing machine (KINGSLH ZX-08, China) for 10 min and then passed through a 60 mesh sieve. Finally, the fine corn stovers were stored in a Ziploc for further experiments at room temperature.

All chemicals used were of analytical reagent grade. A stock solution of Cr(VI) at 100 mg/L concentration was prepared by dissolving  $\text{K}_2\text{Cr}_2\text{O}_7$  in distilled water. Further working solutions were obtained by an appropriate dilution. The solution pH was adjusted with 0.1 M HCl and 0.1 M NaOH solutions.

## 2.2. Sample preparation

To increase the applicability of the composite, three kinds of materials (dolomite, montmorillonite, and corn stover) were manually blended adequately at 5:3:1 (w/w/w). Distilled water was added until the desired moisture level was reached. About 30% montmorillonite was preliminarily determined to be the best proportion for promoting adhesiveness to a raw material during pelletization. The paste was then divided and kneaded into granules 2–3 mm in diameter. After preparation, these samples were dried in an electric oven at  $105 \pm 2^\circ\text{C}$  for 24 h. The dried samples were calcined in a muffle furnace for 1 h at  $600^\circ\text{C}$  to avoid destruction of the particles in water afterwards. The samples were then naturally cooled to room temperature for further study. Photographs of the calcined composite are shown in Fig. 1.

## 2.3. Adsorption experiments

Adsorption experiments were carried out in a 250 mL glass-stoppered conical flask with 100 mL of solution. To assess the effect of composite dosage on removal efficiency, batch studies were performed by changing the composite amount with the range of 0.5–3.0 g. The initial solution pH ranging from 2.0 to 11.0 was adjusted using 0.1 M HCl and 0.1 M NaOH while keeping the initial Cr(VI) concentration at 10 mg/L. The adsorption experiment was conducted at room temperature ( $20 \pm 2^\circ\text{C}$ ). The adsorption kinetics of chromium was investigated with an initial Cr(VI) concentration of 10 mg/L at  $20 \pm 2^\circ\text{C}$ . A composite dosage of 2.0 or 3.0 g was added to 100 mL of Cr(VI) solution for 72 h. For the adsorption isotherm study, 3.0 g of composite was placed in 100 mL of Cr(VI) solution with the initial concentration varied from 5 to 30 mg/L. The equilibrium isotherms were investigated for 72 h at 20, 30, and  $40^\circ\text{C}$ , respectively.

The amount of Cr(VI) removed at any time per unit mass of the composite was evaluated using Eq. (1) [27]:

$$q_t = (C_0 - C_e) V/m \quad (1)$$

The removal efficiency of Cr(VI) from the aqueous was calculated from Eq. (2) [27]:

$$R (\%) = (C_0 - C_e)/C_0 \times 100\% \quad (2)$$

where  $q_t$  (mg/g) is the amount of adsorbed Cr(VI) at any time  $t$ ;  $R$  is the removal efficiency;  $C_0$  and  $C_e$  (mg/L) are the concentrations of Cr(VI) at initial

and equilibrium, respectively;  $m$  (g) is the mass of composite used; and  $V$  (L) is the solution volume.

## 2.4. Analytical methods

Cr(VI) concentration in the solution was determined with a UV–visible spectrophotometer (Hach DR/5000, USA) using diphenylcarbazide solution at a wavelength of 540 nm. A digital standard pH meter was used for pH measurements (ORION 8157BNUMD, USA). Surface morphology was determined with a scanning electron microscopy (SEM) system and energy-dispersive X-ray spectroscopy (EDS) detector (Shimadzu SSX-550, Japan).

## 3. Results and discussion

### 3.1. Characterization of the composite

The prepared dolomite–montmorillonite–corn stover composite is gray colored and 2–3 mm in diameter (shown in Fig. 1(a)). Few particles with black color may be due to high-temperature calcinations of corn stover. The EDS patterns of the calcined composite were shown in Fig. 1(b). The main chemical composition of calcined composite includes C (10.2%), O (49.8%), Mg (20.8%), Al (1.6%), Si (6.8%), and Ca (10.8%). Fig. 1(c) and (d) shows the images of samples before and after Cr(VI) adsorption experiments. Samples after adsorption were collected and dried in an electric oven at  $105 \pm 2^\circ\text{C}$  for 24 h. Fig. 1(c) shows that the samples have a considerably rough surface and complex porous texture that provided more active sites in the course of removal. This complex porous texture can be explained by the calcinations of certain inorganic and organic substances (such as corn stover) during the composite preparation according to Chen et al. [24]. In contrast, Fig. 1(d) reveals that the composite surface significantly changed with the coverage of pores after reaction between the solid and solution system. Most of the open pores are covered by layered crystals. This phenomenon can be attributed to Cr(VI) adsorbed onto the active sites and the solvent-induced morphology change [17].

### 3.2. Effect of composite dosage

Dosage is an important parameter affecting adsorption. The effect of composite amount on removal efficiency was investigated at an initial Cr(VI) concentration of 10 mg/L with dosages varied from 0.5 to 3.0 g/100 mL. As shown in Fig. 2, the highest Cr(VI) removal efficiency was obtained at a dosage of 3.0 g. The removal efficiency of Cr(VI) was found to

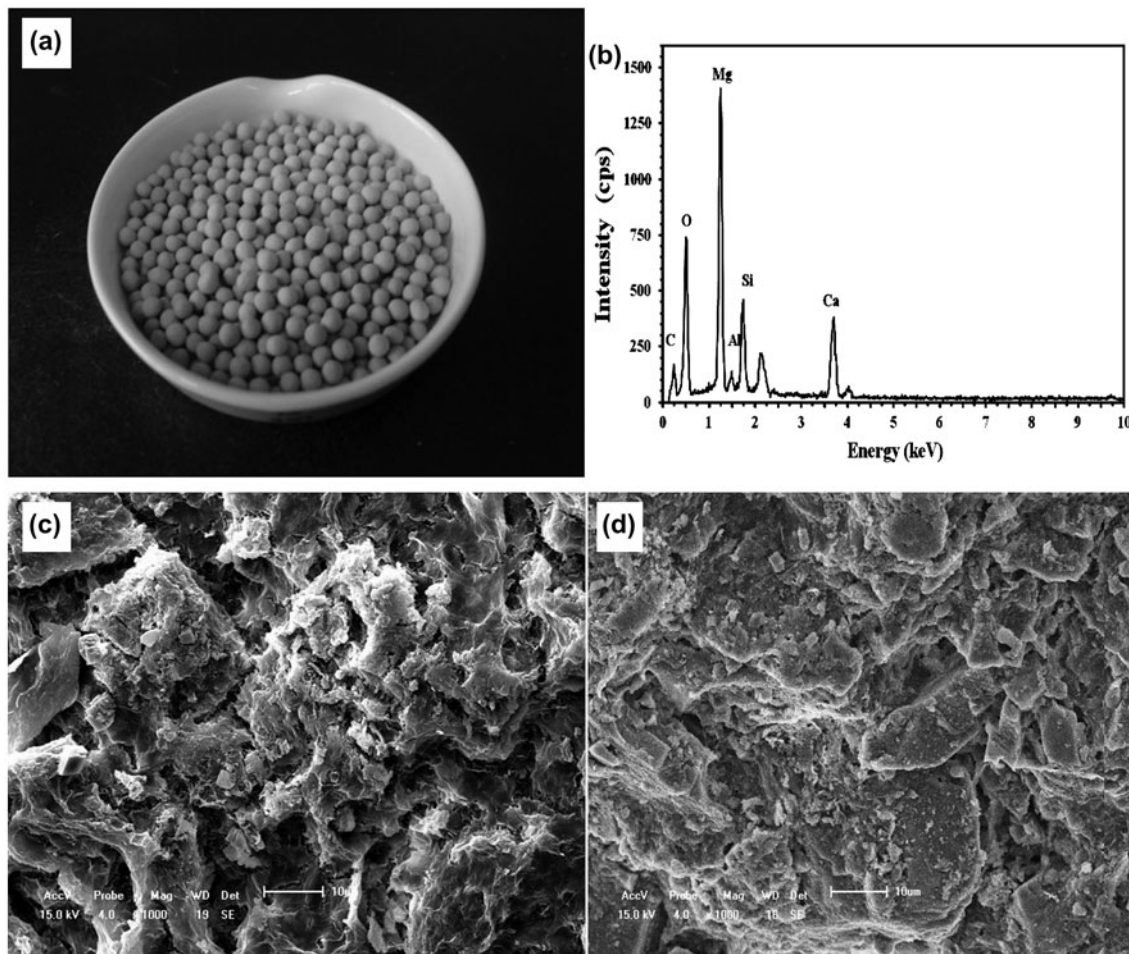


Fig. 1. (a) Photograph of the calcined composite. (b) EDS of the calcined composite. SEM images of the (c) original ( $\times 1,000$ ) and (d) treated composites ( $\times 1,000$ ).

be 58% for 0.5 g/100 mL of composite. It greatly increased to 86% for 2.0 g/100 mL. However, it has been observed that there was only a slow change in the removal efficiency of Cr(VI), when the composite dosage was over 2.0 g/100 mL. Furthermore, higher adsorption dosage result in lower adsorption capacity ( $q_e = 0.3$  mg/g at 3.0 g/100 mL dosage for the composite), as shown in Fig. 2.

The removal efficiency apparently increased with increased composite dosage. This finding can be attributed to the fact that increased dosage increased surface areas and guaranteed a large number of active sites. However, the magnitude of removal capacity decreased with increased composite dosage because of the splitting effect reported by Rathinam et al. [28]. At low dosage, most of active sites are exposed and the adsorption on the surface of the composite is saturated fast, showing a much higher  $q_e$  value. However, at higher composite dosage, the increased mass of

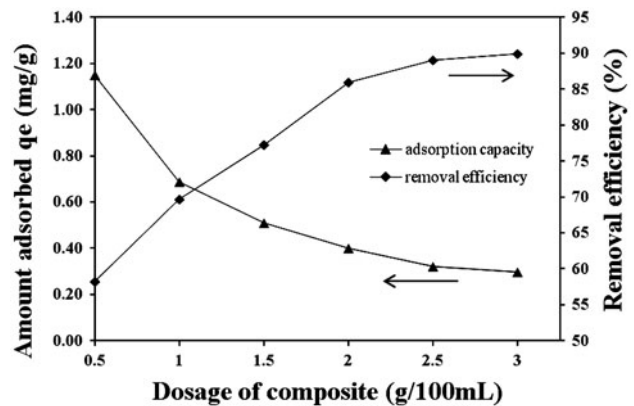


Fig. 2. Removal efficiency of Cr(VI) ions by the composite at an initial Cr(VI) concentration of 10 mg/L with dosages varying from 0.5 to 3 g/100 mL.

adsorbed Cr(VI) cannot catch up with the increased mass of adsorbent. Thus, the concentration gradient



between sorbate and sorbent may cause a decrease in the amount of Cr(VI) adsorbed onto a unit mass of composite with increased composite concentration. In other words, the initial Cr(VI) concentration was kept constant so that it can uptake only a certain amount of active sites on the composite surface. As a result, redundant active sites caused by the increased dosage were rarely occupied by Cr(VI) ions. A corresponding adsorbent dosage exists for each initial ion concentration at which adsorption equilibrium is established according to Uysal and Ar [29]. On the other hand, mutual contact between each composite, to some extent, may decrease the amount of adsorption sites which affected mass transfer process.

### 3.3. Effect of pH

The effect of pH on Cr(VI) removal from a synthetic solution is presented in Fig. 3. The removal efficiency of Cr(VI) at equilibrium increased slightly from 84–86% within pH 2.0–11.0. At pH 2.0–6.0, the predominant Cr(VI) species existed in solution as  $\text{HCrO}_4^-$  and was then gradually converted to  $\text{CrO}_4^{2-}$  until pH increased to 11.0 [30,31]. Results indicated that the removal capability of the composite was nearly independent of the solution pH within the range of 2.0–11.0.

This phenomenon differed from a previous report indicating that the best removal efficiency is obtained within pH 2.0–6.0. In previous research, it has been found that the adsorption ability of Cr(VI) onto both raw montmorillonite and calcined montmorillonite was not quite remarkable and the experimental data of nature and calcined montmorillonite was not shown

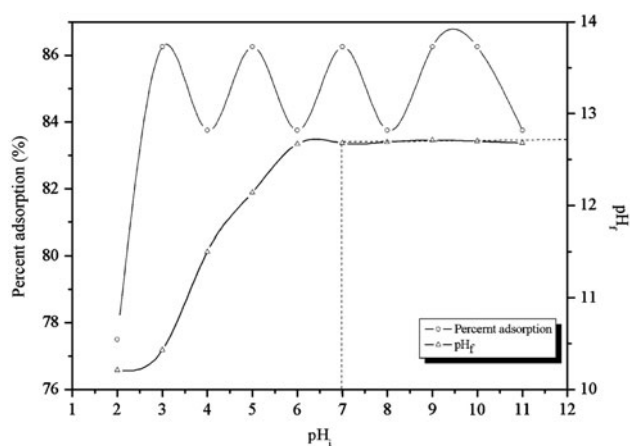


Fig. 3. Effect of solution pH (2.0–11.0) on the removal of Cr(VI) by the composite at an initial Cr(VI) concentration of 10 mg/L at a dosage of 3 g/100 mL.

in this paper. Also, the nature montmorillonite surface is negative charged, thereby it is difficult to adsorb anionic Cr(VI). The point of zero charge ( $\text{pH}_{\text{PCZ}}$ ) for raw dolomite was 8.55, which indicated that the dolomite surface was positively charged at  $\text{pH} < 8.55$ . Electrostatic attraction laws dictate that this phenomenon promotes Cr(VI) adsorption ability with decreased solution pH [17]. However, Staszczuk et al. [32] reported that the physicochemical properties of thermally modified dolomite significantly differ from those of a raw material, such as specific surface area and adsorption capacity. Boucif et al. [33] reported that calcined dolomite at a high temperature generates a large number of positively charged active sites ascribed to the thermal decomposition of dolomite. Karaca et al. [34] also observed pH independency during phosphate adsorption from aqueous solution using calcined dolomite. The effect of pH on phosphate removal is reportedly related to the dissolution of  $\text{Ca}^{2+}$  ions from calcined dolomite and to the polyprotic nature of phosphate ions. Our results can be explained by considering the change in surface charge and competing effects between  $\text{H}^+/\text{OH}^-$  and Cr(VI) ion. On one hand, calcination process may promote the  $\text{pH}_{\text{PCZ}}$  of this composite compared with raw dolomite. As shown in Fig. 3, the point of zero charge was determined as 12.65 according to Chen's report [24]. Therefore, the surface characteristic of the composite is positive at  $\text{pH}_f < 12.65$ , neutral at  $\text{pH}_f = 12.65$ , and negative at  $\text{pH}_f > 12.65$ . The removal efficiency changed slightly is probably due to the higher PZC. On the other hand, with decreased solution pH, the positively charged surface sites formed on the composite can favor the adsorption of Cr(VI) as a result of electrostatic attraction. With increased pH, the concentration of  $\text{OH}^-$  that competed with  $\text{CrO}_4^{2-}$  increased.

### 3.4. Adsorption kinetics

Kinetic tests were conducted under the described condition of sampling for 6 h per sample until the equilibrium point was reached. Cr(VI) uptake at any time  $q_t$  (mg/g) was calculated using Eq. (1).

Pseudo-first-order and pseudo-second-order kinetic models were applied to study the kinetics of removal utilizing following Eqs. (3) and (4) [27]:

$$\ln(q_e - q_t) = \ln q_e - k_1 t \quad (3)$$

$$t/q_t = 1/(k_2 q_e^2) + t/q_e \quad (4)$$

where  $q_e$  and  $q_t$  (mg/g) are the amounts of adsorbate adsorbed at equilibrium and any time  $t$  (h),

respectively;  $k_1$  (1/h) and  $k_2$  (g/mg h) are the adsorption rate constants of the pseudo-first-order and the pseudo-second-order models, respectively.  $k_1$ ,  $k_2$ , and  $q_e$  can be calculated from the slopes and intercepts of the plots (Fig. 4). The experimentally determined ( $q_{e(\text{exp})}$ ) and calculated ( $q_{e(\text{cal})}$ )  $q$  values, correlation coefficients ( $R^2$ ), and kinetic rate constants  $k_1$  and  $k_2$  obtained from the plots for Cr(VI) removal on the composite at 20°C are shown in Table 1.

Comparing the correlation coefficient of the pseudo-first-order model (0.935/0.985) with that of the pseudo-second-order model (0.983/0.991), though both the correlation coefficients were very high, a slight difference indicated that the pseudo-second-order model fitted the data better than the pseudo-second-order model. According to the explanation of Zhao et al's research, in the case of pseudo-second-order kinetic, the calculated  $q_e$  values for the Cr(VI) adsorption on this composite were much closer to the experimental  $q_e$  values and without doubt the adsorption process followed the pseudo-second-order kinetic model [13].

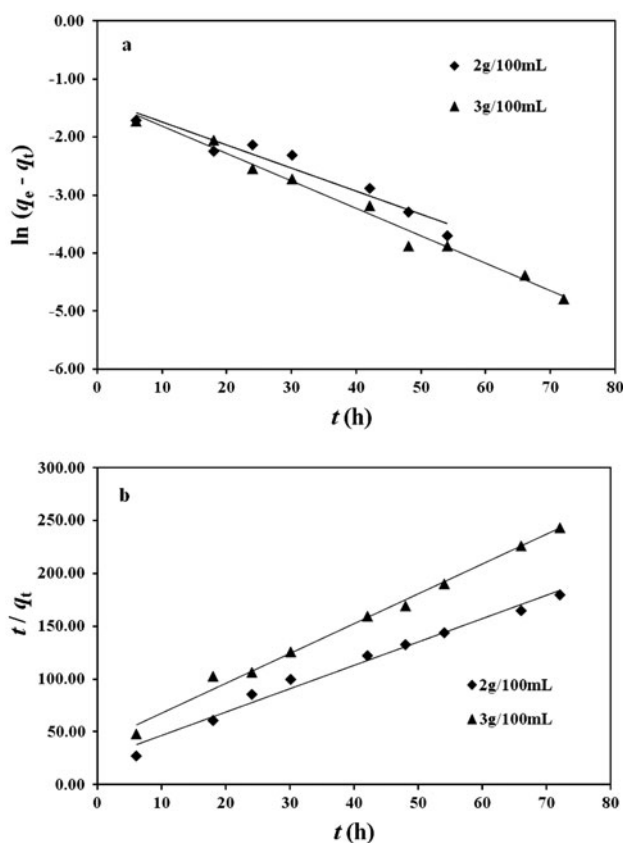


Fig. 4. Kinetic plots of Cr(VI) removal by the composite at different dosages: (a) pseudo-first-order model and (b) pseudo-second-order model at an initial Cr(VI) concentration of 10 mg/L and dosages of 2 or 3 g/100 mL ( $20 \pm 2^\circ\text{C}$ ).

To investigate the adsorption mechanism, the kinetic experimental results were further analyzed with the intraparticle diffusion model. The adsorption mechanism followed a three-stage process: (1) film diffusion, which meant the transportation of the adsorbate to the external surface of the adsorbent from the solution; (2) intraparticle diffusion, which involved the movement of adsorbate within the adsorbent pores; and (3) ion binding on active sites. The third stage was rapid and was not the rate-determining step in adsorbate uptake [17,35]. The overall rate of adsorption was controlled by the slowest step, so the rate-controlling step may either be film or intraparticle diffusion. The intraparticle diffusion rate can be described by the relationship between  $q_t$  and  $t^{0.5}$  using Eq. (5) [36,37]:

$$q_t = k_{p,i} t^{0.5} + C_i \quad (5)$$

where  $k_{p,i}$  ( $\text{mg/g h}^{0.5}$ ) is the intraparticle diffusion rate constant determined from the slope of the plot of  $q_t$  vs.  $t^{0.5}$ ;  $k_{p,i}$  ( $i=1-3$ ) are the three stages of adsorption, respectively; and  $C_i$  ( $\text{mg/g}$ ) is associated with the boundary layer thickness. The rate-controlling step is due only to intraparticle diffusion if the plot is linear and passes through the origin. Otherwise, some other mechanisms along with intraparticle diffusion are also involved.

Fig. 5 shows that the plot was not linear over the entire time range and did not pass through the origin, which implied that the adsorption process was not controlled by intraparticle diffusion. The film diffusion (external surface adsorption) stage finished within 6 h. In addition,  $k_{p,1}$  was much greater than  $k_{p,2}$  and  $k_{p,3}$  from Table 2, and indicated that the external surface adsorption was much faster than intraparticle diffusion. Furthermore,  $C_i \neq 0$  indicated that intraparticle diffusion was not the rate-limiting step [35].

### 3.5. Adsorption equilibrium isotherm

To optimize the design of an adsorption system, the most appropriate correlation for equilibrium curves must be established. In this study, the Langmuir, Freundlich, and Dubinin–Radushkevich (D–R) models were applied to fit the equilibrium data for Cr(VI) removal by the developed composite.

The Langmuir isotherm model assumes that adsorption is a monolayer coverage process and that the maximum adsorption occurs when molecules adsorb onto the surface of a sorbent from a saturated layer [34]. The non-linear and linear forms of the Langmuir equation are given as Eqs. (6) and (7) [3]:

Table 1

The kinetic model constants and coefficients for Cr(VI) removal onto the composite at an initial Cr(VI) concentration of 10 mg/L, 20 ± 2 °C

Dosage (g/100 mL)	$q_{e(\text{exp})}$ (mg/g)	Pseudo-first-order model			Pseudo-second-order model		
		$q_{e(\text{cal})}$ (mg/g)	$k_1$ (1/h)	$R^2$	$q_{e(\text{cal})}$ (mg/g)	$k_2$ (g/mg h)	$R^2$
2.0	0.400	0.258	0.039	0.935	0.434	0.195	0.983
3.0	0.296	0.262	0.047	0.985	0.355	0.198	0.991

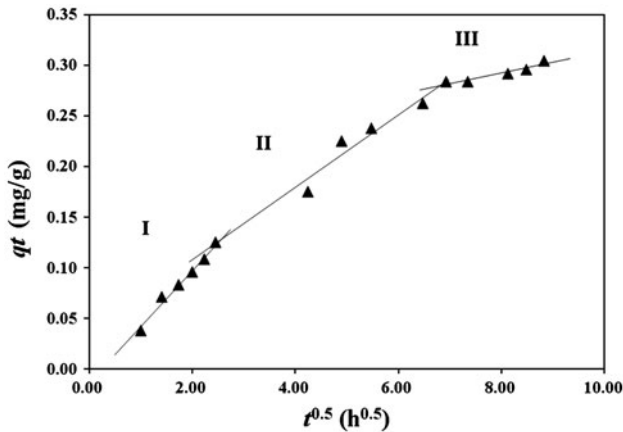


Fig. 5. Plot of intraparticle diffusion model of the removal of Cr(VI) by the composite at a dosage of 3 g/100 mL (20 °C).

Notes: I, film diffusion process; II, intraparticle diffusion process; and III, ion binding on active sites.

$$q_e = K_L Q_0 C_e / (1 + K_L C_e) \tag{6}$$

$$1/q_e = 1/Q_0 + 1/(K_L Q_0 C_e) \tag{7}$$

where  $Q_0$  (mg/g) is the adsorption capacity and  $K_L$  (L/mg) is the adsorption intensity related to the adsorption energy.

The Freundlich isotherm model is based on the assumption that the adsorbent surface energy is heterogeneous and adsorption is multilayered, as expressed by non-linear form Eq. (8) and linear form Eq. (9) [3]:

$$q_e = K_F C_e^{1/n} \tag{8}$$

$$\ln q_e = \ln K_F + 1/n \ln C_e \tag{9}$$

where  $1/n$  is the measure of adsorption intensity or surface heterogeneity.  $K_F$  (mg/g (L/mg)<sup>1/n</sup>) is the constant related to adsorption capacity.

The D–R isotherm is limited to a range of low sorbate concentrations and is used to explain the energetic heterogeneity of a solid surface at the monolayer region in micropores. The equation can be presented as Eq. (10) [35]:

$$q_e = q_e \exp(-K_{DR} \varepsilon^2) \tag{10}$$

where  $q_s$  (mg/g) is the maximum Cr(VI) adsorption capacity for the D–R model,  $K_{DR}$  (mol<sup>2</sup>/kJ<sup>2</sup>) is the adsorption energy constant, and  $\varepsilon$  is the Polanyi potential. The Polanyi potential equals Eq. (11) [35]

$$\varepsilon = RT \ln [1 + 1/C_e] \tag{11}$$

where  $R$  is the gas constant (kJ/mol/K) and  $T$  is the Kelvin temperature (K). The values of  $q_s$  and  $K_{DR}$  were obtained from the plot of  $\ln q_e$  vs.  $\varepsilon^2$ . The adsorption energy  $E$  (kJ/mol) can be calculated by Eq. (12) [35]:

$$E_{DR} = 1/(2K_{DR})^{1/2} \tag{12}$$

where  $E$  (kJ/mol) is the mean free energy of adsorption, which means that the free energy changes when one mole of an ion is transferred from a solution onto the sorbent surface.

The fitting values of the three models of along with regression coefficients ( $R^2$ ) are listed in Table 3. The

Table 2

Intraparticle diffusion model constants and coefficients for Cr(VI) removal onto the composite at an initial Cr(VI) concentration of 10 mg/L, dosage of 3 g/100 mL, 20 ± 2 °C

$k_{p,1}$ (mg/g h <sup>0.5</sup> )	$R^2$	$k_{p,2}$ (mg/gh <sup>0.5</sup> )	$R^2$	$k_{p,3}$ (mg/gh <sup>0.5</sup> )	$R^2$
0.055	0.979	0.035	0.965	0.010	0.918

Table 3

Langmuir, Freundlich, and D–R isotherm model constants and correlation coefficients for adsorption of Cr(VI) onto the composite material at an initial Cr(VI) concentration of 10 mg/L, dosage of 3 g/100 mL, 20, 30, and 40 ± 2 °C

T (K)	Langmuir isotherm			Freundlich isotherm			D–R isotherm			
	Q <sub>0</sub> (mg/g)	K <sub>L</sub> (L/mg)	R <sup>2</sup>	1/n	K <sub>F</sub> (mg/g (L/mg) <sup>1/n</sup> )	R <sup>2</sup>	K <sub>DR</sub> (mol <sup>2</sup> /KJ <sup>2</sup> )	q <sub>s</sub> (mg/g)	E (kJ/mol)	R <sup>2</sup>
293	0.791	0.244	0.952	0.569	0.163	0.936	0.386	0.487	1.138	0.869
303	0.856	0.442	0.947	0.502	0.245	0.935	0.185	0.595	1.644	0.914
313	0.867	0.897	0.976	0.492	0.354	0.960	0.082	0.630	2.469	0.915

higher correlation coefficient calculated by the Langmuir isotherm than that by the Freundlich and D–R models indicated that Cr(VI) was removed mainly in the form of monolayer coverage on the composite surface. Mulange and Garbers-Craig reported similar results for the stabilization of Cr(VI) ions onto exfoliated vermiculite [27]. Q<sub>0</sub> values increased from 0.791 to 0.867 mg/g with increased temperature, which revealed that higher temperatures favored adsorption. Increased K<sub>L</sub> vs. temperature showed that the bond was weak at low temperatures, which further confirmed that high temperatures benefited the removal process. Meanwhile, the large K<sub>L</sub> value suggested the stability of the Cr(VI)-loaded composites, which can be attributed to the existence of chemical bonding forces between Cr(VI) anions and the composite surface [3].

The non-linear plot of the Langmuir and Freundlich isotherms along with the experimental data isotherm is shown in Fig. 6. R<sup>2</sup> calculated by fitting these two non-linear models are 0.9905 and 0.9647, respectively. The maximum adsorption capacity Q<sub>0</sub> and Langmuir constant K<sub>L</sub> of the composite were found to be 0.91 mg/g and 0.22 L/g, respectively. Constants related to the adsorption capacity K<sub>F</sub> and adsorption intensity 1/n were found to be 0.19 and 0.54, respectively. While the value of 1/n is between 0 and 1, the adsorption process of Cr(VI) onto this composite under conducted conditions was favorable according to Mulange and Garbers-Craig's report [27]. One of the important assumptions in the Langmuir isotherm system is the homogeneity of the adsorbent surface [38]. Therefore, this kind of composite may have a homogeneous surface in terms of surface charge distribution [35,39].

In addition, the value of 1/n obtained from the Freundlich isotherm model was found to be <1.0, which indicated that adsorption was favorable [17]. The D-R model was also applied in the form of a linear equation, as shown in Table 3. The adsorption energy values calculated for Cr(VI) were 1.138, 1.644, and 2.469 kJ/mol for the three temperatures, respectively.

The magnitude of E was useful for estimating the mechanism of sorption reaction. At E < 8.0 kJ/mol, physical forces may affect adsorption [40].

### 3.6. Adsorption thermodynamics

Investigation of adsorption thermodynamics is an essential method of determining whether a process is spontaneous. The Gibbs free energy change (ΔG) of adsorption on the composite is related to the distribution coefficient K<sub>d</sub> (the ratio of the amount of removed Cr(VI) to the equilibrium Cr(VI) solution concentration) by Eq. (13) [41]:

$$\ln K_d = -\Delta G/RT \quad (13)$$

where R and T are the gas constant (8.314 J/mol K) and Kelvin temperature, respectively.

ΔG is also related to ΔH and ΔS, which represent changes in enthalpy and entropy, respectively, as expressed in Eq. (14) [41]:

$$\Delta G = \Delta H - T\Delta S \quad (14)$$

Thus, ΔH and ΔS can be obtained from the slope and intercept when ΔG is linearly regressed against T.

The calculated values of ΔH, ΔS, and ΔG for the adsorption of Cr(VI) onto the composite material are listed in Table 4. The obtained positive ΔH values indicated that adsorption was endothermic in nature. The positive values of ΔS reflected increased randomness at the solid/solution interface in the course of removal. Negative values of ΔG indicated weak net attractive interactions and spontaneous adsorption. Generally, the absolute magnitude of the change in free energy for physisorption was between –20 and 0 kJ/mol and chemisorption ranged from –80 to –400 kJ/mol [42]. Hence, this process may be considered as physisorption. Similar findings have been reported by Hamadi et al. [1].



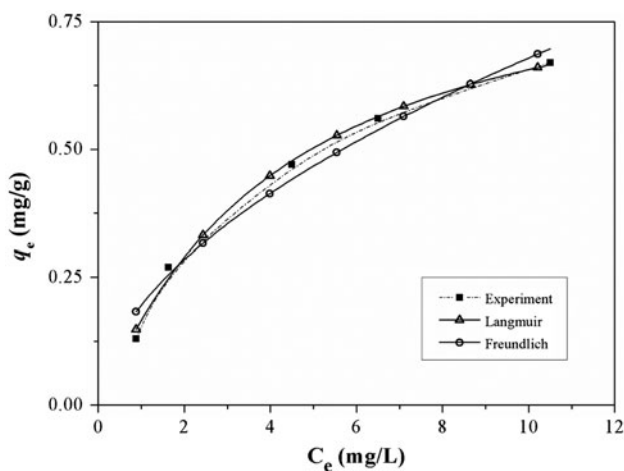


Fig. 6. Plot of non-linear isotherm model of the removal of Cr(VI) by the composite at an initial Cr(VI) concentration of 10–50 mg/L at a dosage of 3.0 g/100 mL (20 °C).

### 3.7. Regeneration of the synthesized composite

Regeneration of the synthesized composite is vital if it is to be utilized for treatment of contaminated water. The adsorbed composite was regenerated by several concentration of NaOH solution from 0, 0.01,

0.1, 0.5, and 1 M. The recovery efficiency of different concentration of NaOH solution was 0, 8, 27, 59, and 84%, respectively. The result demonstrated that NaOH solutions exhibited effectively for displacing Cr(VI) anions from the composite. This might be caused by the stronger binding power between  $\text{OH}^-$  and the positive charged composite surface than those with Cr(VI) anions.

### 3.8. Comparison of Cr(VI) adsorption capacities of various mineral adsorbents

The adsorption capacity of the synthesized composite in this study was compared with other mineral adsorbents reported in literature as shown in Table 5. Our present study reports 1.15 mg/g of Cr(VI) adsorption by using this synthesized composite which is comparatively low. Nevertheless, it is worthwhile mentioning that a critical direct comparison of the capacity of the adsorbents is difficult due to the different operating conditions such as pH, dosage of the adsorbent, initial concentration. But a major point worth noting is that the range of pH for Cr(VI) removal is considerably wider as compared to other reported methods, thus demonstrating the application possibility of this synthesized composite.

Table 4

Thermodynamic parameters for Cr(VI) removal onto the composite at the initial concentration varying from 5, 10, 15, 20, and 30 mg/L, dosage of 3 g/100 mL,  $20 \pm 2^\circ\text{C}$

Concentration of Cr(VI) (mg/L)	$\Delta H$ (kJ/mol)	$\Delta S$ (kJ/mol K)	$\Delta G$ (kJ/mol)		
			293 K	303 K	313 K
5	53.34	0.194	-3.705	-5.467	-7.596
10	49.85	0.183	-3.921	-5.836	-7.593
15	48.43	0.171	-2.005	-3.180	-5.436
20	44.54	0.157	-1.735	-2.729	-4.880
30	30.14	0.108	-1.570	-2.418	-3.729

Table 5

Summary of Cr(VI) adsorption capacities of various mineral adsorbents

Mineral adsorbents	Adsorption capacity (mg/g)	Reference
Volcanic rocks	0.046	[43]
Vermiculite	0.263	[20]
Fe(III)-coated natural zeolite	0.4–0.7	[41]
Calcined bauxite	2.0	[44]
Bentonite	5.9	[45]
The synthesized composite	1.15	This study

#### 4. Conclusions

The effects of parameters such as composite dosage, solution pH, contact time, initial concentration, and temperature on Cr(VI) removal from an aqueous solution were investigated. Experimental results revealed that this composite developed from a mixture of dolomite–montmorillonite–corn stover was effective for Cr(VI) removal from an aqueous solution. The maximum Cr(VI) removal efficiency was found to be approximately 90% at a dosage of 3.0 g/100 mL with an initial Cr(VI) concentration of 10 mg/L after 72 h. The removal procedure was observed to be independent from the solution pH because the removal efficiency was almost unchanged with the pH range of 2.0–11.0. The removal efficiency showed a sharp increase with increased temperature. Cr(VI) removal by the composite followed a pseudo-second-order kinetic model. The experimental data were fitted to the intraparticle diffusion model to discuss the removal mechanism, which demonstrated that the film diffusion rate was fast and the intraparticle diffusion was not the rate-limiting step during the removal process. The removal process also well fitted the Langmuir isotherm model, which indicated that Cr(VI) ions were mainly adsorbed in the form of monolayer coverage on the composite surface. The D–R isotherm model revealed that physical forces may affect sorption. Thermodynamic data indicated that the removal process was endothermic in nature and spontaneous.

#### Acknowledgements

The authors thank the “Beijing National Science Foundation (8144053)”, the National Natural Science Foundation of China (NSFC) (21407129), and the “Fundamental Research Funds for the Central Universities (2652013025)” for financial support for this work.

#### References

- [1] N.K. Hamadi, X.D. Chen, M.M. Farid, M.G.Q. Lu, Adsorption kinetics for the removal of chromium(VI) from aqueous solution by adsorbents derived from used tyres and sawdust, *Chem. Eng. J.* 84 (2001) 95–105.
- [2] A. Gładysz-Płaska, M. Majdan, D. Sternik, S. Pikus, E. Zięba, Sorptive and thermal properties of red clay in relation to Cr(VI), *J. Therm. Anal. Calorim.* 101 (2010) 775–778.
- [3] Y.B. Zeng, H. Woo, G. Lee, J. Park, Adsorption of Cr(VI) on hexadecylpyridinium bromide (HDPB) modified natural zeolites, *Microporous Mesoporous Mater.* 130 (2010) 83–91.
- [4] F. Xu, T. Ma, A. Ellis, C.F. Liu, Y.J. Gao, L. Li, Biogeochemical processes of chromium stable isotope in groundwater, *Earth Sci. Front.* 19 (2012) 183–193.
- [5] B.R. James, R.J. Bartlett, Plant-soil interactions of chromium, *J. Environ. Qual.* 13 (1984) 67–70.
- [6] S. Itoh, H. Shimada, Clastogenicity and mutagenicity of hexavalent chromium in *lacZ* transgenic mice, *Toxicol. Lett.* 91 (1997) 229–233.
- [7] Guidelines for Drinking-water Quality, fourth ed., World Health Organisation, Geneva, 2011.
- [8] S.K. Sharma, B. Petrusevski, G. Amy, Chromium removal from water: A review, *J. Water Supply: Res. Technol.* 57 (2008) 541–554.
- [9] A.J. Chaudhary, N.C. Goswami, S.M. Grimes, Electrolytic removal of hexavalent chromium from aqueous solutions, *J. Chem. Technol. Biotechnol.* 78 (2003) 877–883.
- [10] C. Barrera-Díaz, M. Palomar-Pardavé, M. Romero-Romo, S. Martínez, Chemical and electrochemical considerations on the removal process of hexavalent chromium from aqueous media, *J. Appl. Electrochem.* 33 (2003) 61–71.
- [11] B. Galán, D. Castañeda, I. Ortiz, Removal and recovery of Cr(VI) from polluted ground waters: A comparative study of ion-exchange technologies, *Water Res.* 39 (2005) 4317–4324.
- [12] A. Hafiane, D. Lemordant, M. Dhabbi, Removal of hexavalent chromium by nanofiltration, *Desalination* 130(3) (2000) 305–312.
- [13] Y.X. Zhao, S.J. Yang, D.H. Ding, J. Chen, Y.N. Yang, Z.F. Lei, C.P. Feng, Z.Y. Zhang, Effective adsorption of Cr(VI) from aqueous solution using natural Akadama clay, *J. Colloid. Interface Sci.* 395 (2013) 198–204.
- [14] A. Sari, M. Tuzen, Removal of Cr(VI) from aqueous solution by Turkish vermiculite: Equilibrium, thermodynamic and kinetic studies, *Sep. Sci. Technol.* 43 (2008) 3563–3581.
- [15] K.G. Bhattacharyya, S.S. Sen Gupta, Adsorption of chromium(VI) from water by clays, *Ind. Eng. Chem. Res.* 45 (2006) 7232–7240.
- [16] B.S. Krishna, D.S.R. Murty, B.S. Jai Prakash, Thermodynamics of chromium(VI) anionic species sorption onto surfactant-modified montmorillonite clay, *J. Colloid. Interface Sci.* 229 (2000) 230–236.
- [17] A.B. Albadarin, C. Mangwandi, A.H. Al-Muhtaseb, G.M. Walker, S.J. Allen, M.N.M. Ahmad, Kinetic and thermodynamics of chromium ions adsorption onto low-cost dolomite adsorbent, *Chem. Eng. J.* 179 (2012) 193–202.
- [18] X.Y. Chuan, X.C. Lu, P. Gong, Installing engineering in micro-structure and photo-catalytic properties of porous mineral, *Earth Sci. Front.* 12(1) (2005) 188–195.
- [19] A.H. Lu, New advances in the study of environmental mineralogical materials: Pollution treatment by inorganic minerals—the fourth category of pollution treatment methods, *Earth Sci. Front.* 12(1) (2005) 196–205.
- [20] K.M.S. Sumathi, S. Mahimairaja, R. Naidu, Use of low-cost biological wastes and vermiculite for removal of chromium from tannery effluent, *Bioresour. Technol.* 96 (2005) 309–316.
- [21] E. Pehlivan, A.M. Özkan, S. Dinç, Ş. Parlayıcı, Adsorption of Cu<sup>2+</sup> and Pb<sup>2+</sup> ion on dolomite powder, *J. Hazard. Mater.* 167 (2009) 1044–1049.
- [22] S. Karaca, A. Gürses, M. Ejder, M. Açıkıldız, Kinetic modeling of liquid-phase adsorption of phosphate on dolomite, *J. Colloid. Interface Sci.* 277 (2004) 257–263.

- [23] G.M. Ayoub, M. Mehawej, Adsorption of arsenate on untreated dolomite powder, *J. Hazard. Mater.* 148 (2007) 259–266.
- [24] N. Chen, Z.Y. Zhang, C.P. Feng, D.R. Zhu, Y.N. Yang, N. Sugiura, Preparation and characterization of porous granular ceramic containing dispersed aluminum and iron oxides as adsorbents for fluoride removal from aqueous solution, *J. Hazard. Mater.* 186 (2011) 863–868.
- [25] C.P. Liao, Y.J. Yang, C.Z. Wu, H.T. Huang, Study on the distribution and quantity of biomass residues resource in China, *Biomass Bioenergy* 27 (2004) 111–117.
- [26] A. Salem, R. Akbari Sene, Removal of lead from solution by combination of natural zeolite-kaolin-bentonite as a new low-cost adsorbent, *Chem. Eng. J.* 174 (2011) 619–628.
- [27] D.M. Mulange wa Mulange, A.M. Garbers-Craig, Stabilization of Cr(VI) from fine ferrochrome dust using exfoliated vermiculite, *J. Hazard. Mater.* 223–224 (2012) 46–52.
- [28] A. Rathinam, B. Maharshi, S.K. Janardhanan, R.R. Jonnalagadda, B.U. Nair, Biosorption of cadmium metal ion from simulated wastewaters using *Hypnea valentiae* biomass: A kinetic and thermodynamic study, *Bioresour. Technol.* 101 (2010) 1466–1470.
- [29] M. Üysal, I. Ar, Removal of Cr(VI) from industrial wastewaters by adsorption, *J. Hazard. Mater.* 149 (2007) 482–491.
- [30] J. Hu, G.H. Chen, I.M.C. Lo, Removal and recovery of Cr(VI) from wastewater by maghemite nanoparticles, *Water Res.* 39 (2005) 4528–4536.
- [31] A. Nakajima, Y. Baba, Mechanism of hexavalent chromium adsorption by persimmon tannin gel, *Water Res.* 38 (2004) 2859–2864.
- [32] P. Staszczuk, E. Stefaniak, B. Biliński, E. Szymański, R. Dobrowolski, S.A.A. Jayaweera, Investigations on the adsorption properties and porosity of natural and thermally treated dolomite samples, *Powder Technol.* 92 (1997) 253–257.
- [33] F. Boucif, K. Marouf-Khelifa, I. Batonneau-Gener, J. Schott, A. Khelifa, Preparation, characterisation of thermally treated Algerian dolomite powders and application to azo-dye adsorption, *Powder Technol.* 201 (2010) 277–282.
- [34] S. Karaca, A. Gurses, M. Ejder, M. Acikyildiz, Adsorptive removal of phosphate from aqueous solutions using raw and calcinated dolomite, *J. Hazard. Mater.* 128 (2006) 273–279.
- [35] A.B. Albadarin, A.H. Al-Muhtaseb, G.M. Walker, S.J. Allen, M.N.M. Ahmad, Retention of toxic chromium from aqueous phase by H<sub>3</sub>PO<sub>4</sub>-activated lignin: Effect of salts and desorption studies, *Desalination* 274 (2011) 64–73.
- [36] Y.H. Xie, S.Y. Li, G.L. Liu, J. Wang, K. Wu, Equilibrium, kinetic and thermodynamic studies on perchlorate adsorption by cross-linked quaternary chitosan, *Chem. Eng. J.* 192 (2012) 269–275.
- [37] Y. Wu, S.Z. Zhang, X.Y. Guo, H.L. Huang, Adsorption of chromium(III) on lignin, *Bioresour. Technol.* 99 (2008) 7709–7715.
- [38] Y.S. Ho, G. McKay, The kinetics of sorption of divalent metal ions onto sphagnum moss peat, *Water Res.* 34 (2000) 735–742.
- [39] J. Rahchamani, H.Z. Mousavi, M. Behzad, Adsorption of methyl violet from aqueous solution by polyacrylamide as an adsorbent: Isotherm and kinetic studies, *Desalination* 267 (2011) 256–260.
- [40] S. Kushwaha, B. Sreedhar, P.P. Sudhakar, A spectroscopic study for understanding the speciation of Cr on palm shell based adsorbents and their application for the remediation of chrome plating effluents, *Bioresour. Technol.* 116 (2012) 15–23.
- [41] G.X. Du, Z.H. Li, L.B. Liao, R. Hanson, S. Leick, N. Hoepfner, W.T. Jiang, Cr(VI) retention and transport through Fe(III)-coated natural zeolite, *J. Hazard. Mater.* 221–222 (2012) 118–123.
- [42] Y. Yu, Y.Y. Zhuang, Z.H. Wang, Adsorption of water-soluble dye onto functionalized resin, *J. Colloid. Interface Sci.* 242 (2001) 288–293.
- [43] E. Alemayehu, S. Thiele-Bruhn, B. Lennartz, Adsorption behaviour of Cr(VI) onto macro and micro-vesicular volcanic rocks from water, *Sep. Purif. Technol.* 78 (2011) 55–61.
- [44] S.S. Baral, S.N. Das, P. Rath, G.R. Chaudhury, Chromium(VI) removal by calcined bauxite, *Biochem. Eng. J.* 34 (2007) 69–75.
- [45] N. Tewari, B.K. Guha, P. Vasudevan, Adsorption study of hexavalent chromium by bentonite clay, *Asian J. Chem.* 17 (2005) 2184–2190.